CHAPTER 5

A synergistic approach combining Adsorption and Biodegradation for effective treatment of Acid Blue 113 dye by Klebsiella grimontii entrapped Graphene Oxide-Calcium Alginate Hydrogel Beads

CHAPTER 5

A synergistic approach combining Adsorption and Biodegradation for effective treatment of Acid Blue 113 dye by *Klebsiella grimontii* entrapped Graphene Oxide-Calcium Alginate Hydrogel Beads

5.1 Introduction

With the remarkable progress in both biotechnology and nanotechnology, the application of biofunctionalized nanomaterials has emerged as a highly captivating research area for the biotechnological remediation of organic pollutants (Banerjee et al., 2018; Pavlidis et al., 2014). Graphene and Graphene Oxide (GO)-based nanomaterials have recently been the subject of extensive research for their potential use in wastewater treatment due to their unique structures and characteristics (Gan et al., 2015). GO, a two-dimensional carbon backbone from graphene (Sun and Fugetsu, 2014), possess a large surface area and numerous oxygen-containing groups (such as epoxy, carboxyl, ketone, and hydroxyl groups) at its basal planes and edges (Gan et al., 2018). This makes GO an ideal material for developing GO-based polymer hydrogels with enhanced adsorption capabilities and a strong affinity for various organic pollutants (X. Gu et al., 2014; Yuan et al., 2013).

Recently, bio-encapsulation of microbial cells into Graphene Oxide-Calcium alginate (GO-CA) hydrogel beads has been shown effective pollutants degradation from wastewater (Fares et al., 2020; Godiya et al., 2020). Microorganisms could undergo a condition of dormancy in which their cells are alive but uncultivable due to a reduction in their metabolic activity in an environment contaminated with organic pollutants (Jia et al., 2020; Su et al., 2021). However, the entrapment of microbial cells within GO-CA hydrogel beads provides additional benefits, such as increased tolerance against environmental stress, reduced loss of free cells, and low

hydraulic retention time (HRT) (Bustos-Terrones et al., 2022; Y. Wang et al., 2020). Hydrogel beads offer the advantage of enabling the easy adsorption and biodegradation of dyes simultaneously, eliminating the restrictions associated with using individual biodegradation and adsorption methods (Li et al., 2018). The porous structure of KG-GO-CA hydrogel beads enables the diffusion of dye molecules and oxygen from the surrounding liquid layer, allowing entrapped microbial cells to biodegrade the dye molecules, with the resulting metabolites diffusing back to the bulk liquid (Zur et al., 2016) (**Figure 5.1**).

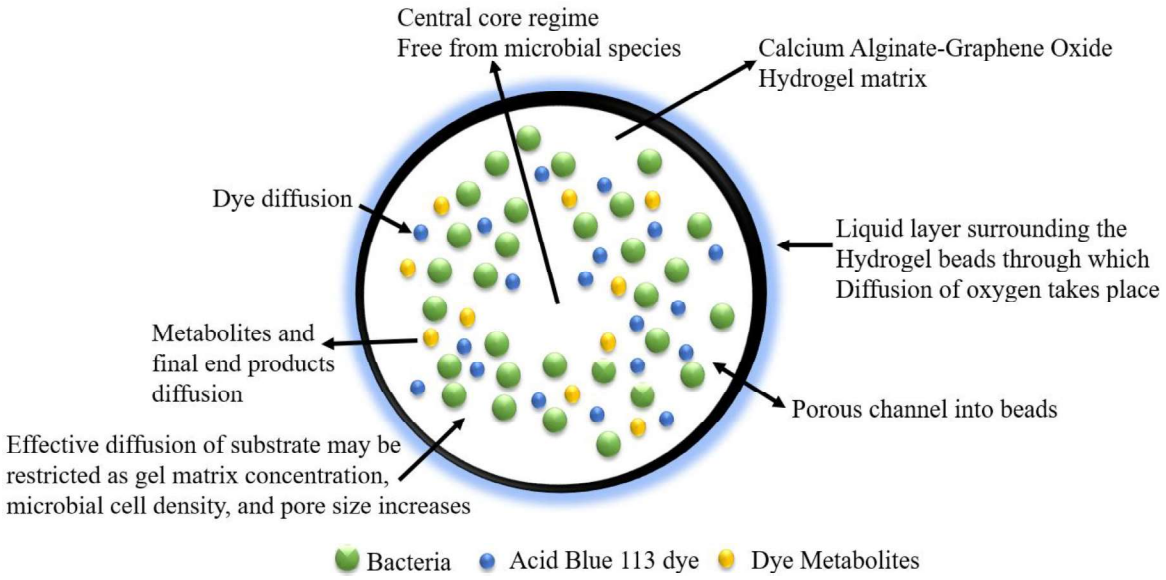

Figure 5.1. Demonstrating the remarkable ability of KG-GO-CA hydrogel beads to facilitate dye diffusion, adsorption, and biodegradation simultaneously

This study investigated the effective mineralization of AB 113 dye-contaminated wastewater using GO-CA bacterial cell-entrapped hydrogel beads. The performance of the designed FBBR system was assessed under various conditions, and the performance of continuous FBBR was elucidated by varying the inlet flow rate and inlet shock loading rates. Moreover, the study examined the reusability of KG-GO-CA hydrogel beads. Further, the bacterial toxicity study was conducted to ensure the safe disposal and application of treated water for commercial and daily purposes.

5.2 Materials and Methods

5.2.1 Dye and Chemicals

The chemicals and dye employed in the present study were procured from Sigma Aldrich (India) and comprised Acid Blue 113 ($C_{32}H_{21}N_5Na_2O_6S_2$) dye, Graphite powder, Sodium Nitrate ($NaNO_3$), Potassium Permanganate ($KMnO_4$), Hydrogen Peroxide (H_2O_2), Sodium Alginate, and Sulfuric Acid (H_2SO_4).

5.2.2 Microorganism

In this study, a potential dye-degrading bacterial species, *Klebsiella grimontii*, was isolated from soil contaminated with textile effluent, as described in section 3.2.2. The phylogenetic tree of bacterial species illustrated in **Figure 5.2**.

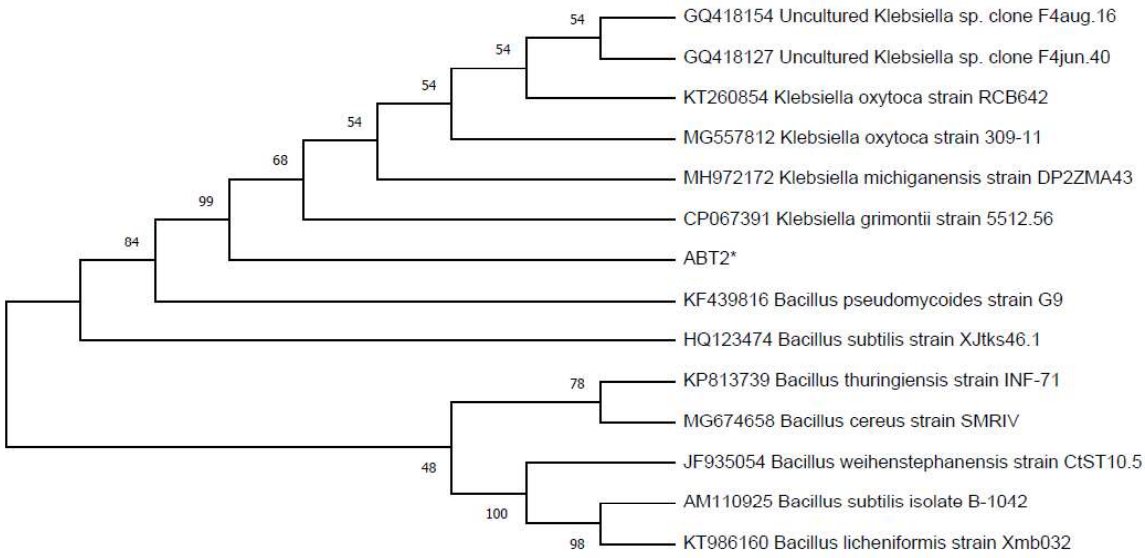

Figure 5.2. Phylogenetic tree of isolated bacterial species *Klebsiella grimontii*

5.2.3 Graphene Oxide (GO) and KG-GO-CA hydrogel beads preparation

Graphene oxide (GO) was prepared using the Modified Hummer's method (Nardjess et al., 2023). Briefly, a mixture of Graphite powder (2.0 g), $NaNO_3$ (2.0 g), and H_2SO_4 (98% purity) (90 mL) was taken in an Erlenmeyer flask under an ice bath (0-5 °C) and mixed for 4 hr.

Further, 12 g of $KMnO_4$ was slowly mixed to oxidize reaction mixture, beside the temperature of the solution should remain below 15 °C, again magnetically stirred for 2 hr. After removing the ice bath, the mixture was heated at 35 °C for 2 hours. Subsequently, 180 mL of distilled water was added to the constantly stirred mixture, and the temperature was raised to 95 °C, avoiding boiling, and maintained for 1 hr to facilitate the exfoliation of GO. The heater was then turned off, and the mixture was allowed to cool to room temperature (27 °C) naturally. Moreover, 100 mL of distilled water was added to the cooled mixture, and the resulting mixture was stirred for an additional 1 hr to ensure thorough dispersion of the GO sheets. Finally, to terminate the reaction, 30% (v/v) H_2O_2 was added to the reaction mixture, ensuring complete oxidation of any remaining unreacted compounds. The mixture was vacuum filtered. The solid residue was oven-dried overnight and followed by pulverization to obtain GO powder.

GO-Calcium Alginate-bacterial cell immobilized hydrogel beads were prepared by adopting the procedure mentioned elsewhere (Chang et al., 1998). Obtained GO powder (1 gm) was dissolved in 100 mL MilliQ water and sonicated (20 kHz) for 20 min. Sodium alginate (SA) (2.5 gm) was gently dissolved in 100 mL MilliQ water. 24 hr overgrown bacterial cell (OD at 600 nm = 1) was centrifuged at 6000 rpm for 10 min and the biomass of the cell culture was dissolved in 2.5 wt % NaCl solution. GO and SA solutions were continuously mixed for 1 hr until became homogeneous and thereafter, the bacterial cell was dissolved in the mixture. The mixture was allowed for 24 hr incubation at 30 °C. Ultimately, the GO-SA bacterial cell mixture was dropwise added to the cross-linker (6% w/v) $CaCl_2$ solution to obtain the GO-Calcium alginate (GO-CA) bacterial cell entrapped hydrogel beads (**Figure 5.3**). The KG-GO-CA hydrogel beads were further soaked in 5% (v/v) HCl to attain stable beads (Sun and Fugetsu, 2014).

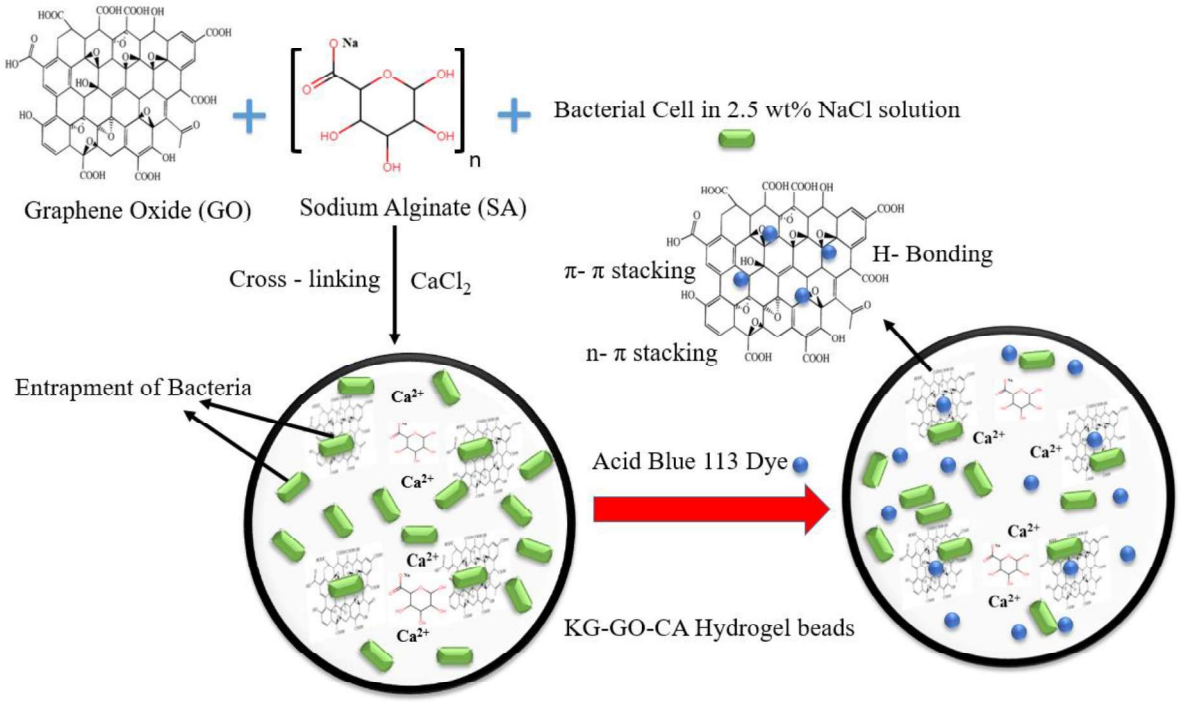

Figure 5.3. Schematic representation of the preparation process for Graphene Oxide-Calcium alginate bacterial cell (*Klebsiella grimontii*) entrapped KG-GO-CA hydrogel beads

The essential feature of immobilization within the alginate beads is to provide favourable microenvironmental conditions (i.e., cell-cell contact, nutrient-product gradients, pH gradients) for cells, resulting in better performance of the biocatalysts (e.g., higher product yields and rates). Moreover, it provides cell reuse and eliminates the costly processes of cell recovery and cell recycle, and improves genetic stability. Thus, the entrapped microbes have successively reused for biosorption experiment. The removal efficiency however declined after successive use, but the cell activity sustained throughout the experiment. The sterilization is not needed after the cell immobilization within the alginate beads. Since the microbial cell activity sustained after the immobilization, and so the biosorption easily facilitated within the Fluidized bed Bioreactor system.

5.3.3 Characterization of GO and KG-GO-CA Hydrogel Beads

The prepared GO and KG-GO-CA hydrogel beads were characterized using various analytical instruments, namely SEM, FTIR, Thermogravimetric Analysis (TGA) (TGA-50, M/s Shimadzu, heating rate 10 °C/min under N_2 environment to 600 °C), and High-Resolution X-Ray Diffraction (HR-XRD) (Rigaku SmartLab 9kW, RIGAKU, 10-80°, 4°/min, $\lambda_{Cu\ K\alpha}$ = 0.15418 nm). TGA is a sophisticated analytical technique used to study the behavior of materials as they are heated or subjected to changing temperatures. The sample's weight is continuously monitored as it is exposed to a controlled temperature increase. It elucidates the material's thermal stability, decomposition patterns, and changes in composition. HR-XRD is used to study the crystallographic structure of materials with exceptional precision. X-rays are directed at a sample, and the resulting diffraction pattern provides detailed information about the arrangement of atoms in the material's lattice structure. The specific surface area of the GO and KG-GO-CA hydrogel beads was determined using N_2 sorption isotherm (77 K) by Brunauer–Emmet–Teller (BET) analysis (MicrotracBEL, 6 hr soak time, target temperature 200 °C with a rate of 2 °C/min). The BET theory assumes that gas molecules form a monolayer on the surface, and this assumption allows for the determination of the specific surface area. The GO particle size distribution and zeta potential were measured using Malvern Panalytical, Zetasizer (MAL1213575).

5.3.4 Fluidized Bed Bioreactor (FBBR)

This study employed a Fluidized Bed Bioreactor (FBBR) made of borosilicate glass with dimensions of 6 cm diameter and 75 cm height. The FBBR had a working volume of 600 mL and was operated in semi-batch mode (**Figure 5.4**). The bioreactor was filled with 20 g of KG-GO-CA hydrogel beads as the active mass. The dye solution was introduced at the bottom port

of the bioreactor, and fluidization was achieved by upward airflow from the bottom. An air pump (Hailea ACO 9601, 2.0 W) was used to produce airflow at a rate of 3.0 ± 1.0 L/min.

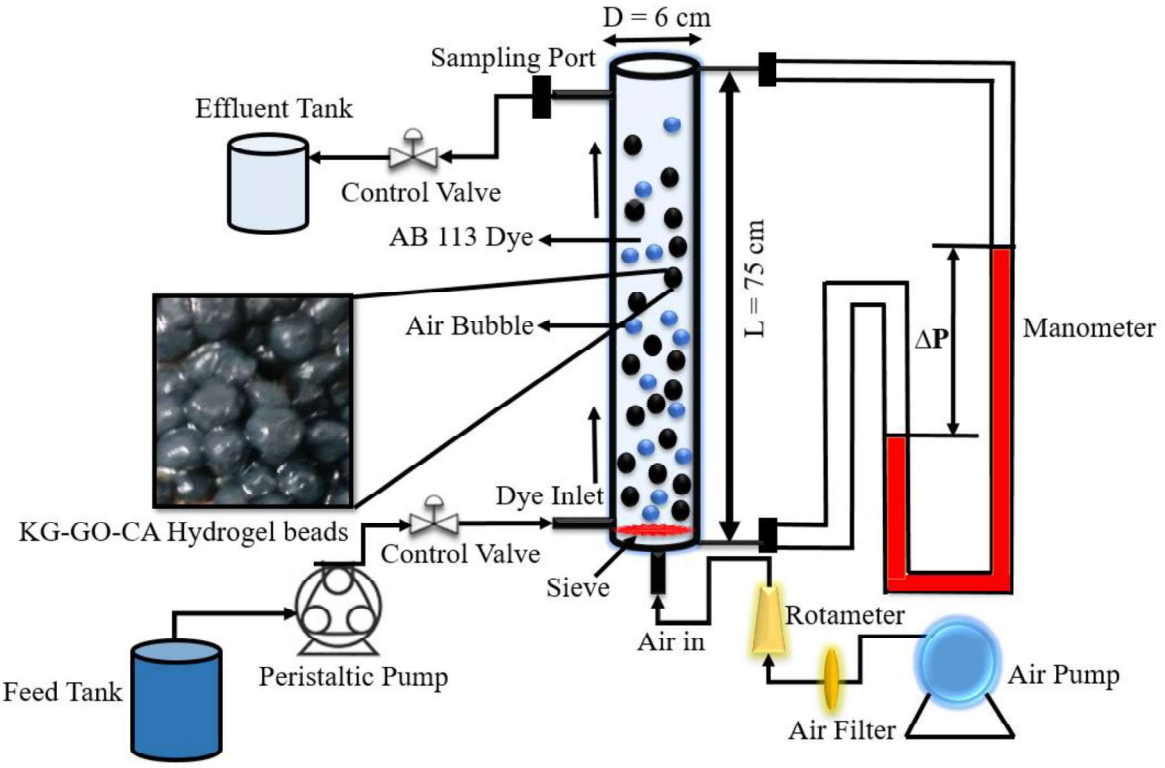

Figure 5.4. Schematic diagram of the laboratory-scale Fluidized Bed Bioreactor (FBBR) used in the study, featuring KG-GO-CA hydrogel beads fluidized with upflowing air and AB 113 dye in Nutrient broth media (30 ± 2.0 °C and pH 7.0± 0.5)

5.3.5 Dissolved Oxygen (DO) and Oxygen uptake rate (OUR) measurement

AB 113 wastewater samples exposed to KG-GO-CA hydrogel beads were aerated for 60 minutes to reach saturation with dissolved oxygen (DO). DO refers to the amount of oxygen molecules that are present in a liquid, typically water. It plays a crucial role in supporting aquatic life and various biochemical processes. The concentration curve of DO was generated by recording DO levels over time. Oxygen Uptake Rate (OUR) is a key parameter used to measure the rate at which microorganisms consume oxygen during their metabolic activities, especially in aerobic biological processes. As microorganisms metabolize organic matter, they

require oxygen as a vital element for their biochemical reactions. OUR can be defined as the oxygen consumed per unit of time, which was calculated using Eq. (5.1):

$$\text{OUR} = \frac{C_2 - C_1}{t_1 - t_2} \tag{5.1}$$

where, C_1 and C_2 are the DO concentration (mg/L) with corresponding time durations of t_1 and t_2, respectively.

5.3.6 Continuous Study in a Fluidized Bed Bioreactor

The performance of the biosorption process, which combines adsorption and biodegradation, was also evaluated in a continuous mode. The FBBR system was designed to allow effective contact between the KG-GO-CA beads and AB 113 wastewater. The inlet volumetric flow rates of AB 113 were varied between 20-80 mL/h at an initial dye concentration of 100 mg/L using a peristaltic pump (ELECTROLAB, PP-50V). The dye removal was monitored continuously for 60 days. The appropriate nutrient and dissolved oxygen (DO) levels were maintained during the biodegradation process. The bioreactor was operated continuously, allowing steady-state conditions to establish in the FBBR. All measurements were performed in triplicate, and their average values were used for data analysis. The AB113 removal performance in continuous FBBR was assessed using the following equations:

$$\text{Inlet shock loading rates (ISLR)} = \frac{C_{in} \times Q}{V} \tag{5.2}$$

$$\text{Dye Removal Efficiency (RE)} = \frac{C_{in} - C_{out}}{C_{in}} \times 100 \tag{5.3}$$

$$\text{Dye Elimination Capacity (EC)} = \frac{(C_{in} - C_{out})}{V} \times Q \tag{5.4}$$

where C_{in} and C_{out} refer to the inlet and outlet concentrations of AB 113, respectively. Q and V stand for the volumetric flow rate (mL/h) and active hold-up volume of FBBR, respectively.

5.3.7 Batch Adsorption Study

Adsorption isotherms study helps to understand the characteristics of adsorption. In this work, Langmuir and Freundlich models were fitted with experimental data to study the adsorption isotherm. Adsorption of AB 113 was carried out by KG-GO-CA hydrogel beads at room temperature with varying dye concentrations of 50-300 mg/L. The adsorption capacity of AB 113 was calculated using the following expression:

$$q_e = \frac{C_0 - C_e}{m} \times V \tag{5.5}$$

where C_0 and C_e are the initial and equilibrium concentrations of AB 113 (mg/L), respectively. q_e, m, and V are the amount of AB 113 adsorbed (i.e., adsorption capacity (mg/g)), the amount of hydrogel beads (g), and the volume of solution (L), respectively.

The adsorption isotherm proposed by Langmuir in 1918 assumes monolayer adsorption with equal and energetically similar adsorption sites. Langmuir adsorption isotherm equation can be stated as:

$$Q_e = Q_m \frac{K_i.\ C_e}{1 + K_i.\ C_e} \tag{5.6}$$

where Q_e is the adsorption capacity at equilibrium (mg/g), C_e is residual AB 113 equilibrium concentration (mg/L), K_i is the constant link with the affinity of the binding sites (L/mg); and Q_m is the amount of AB 113 adsorbed that formed a complete monolayer coverage (mg/g), respectively.

An empirical equation that makes use of multilayer adsorption on a heterogeneous surface is the Freundlich isotherm model. The equation's mathematical form is expressed as follows:

$$Q_e = K_f . C_e^{\frac{1}{n}} \tag{5.7}$$

K_f is the Freundlich constant (L/g) associated with adsorption capacity, an empirical exponent (n) that reflects the heterogeneity of the adsorption sites and the non-uniformity of the surface.

5.3.8 Breakthrough Curve

To perform the fixed bed experiment for the calculation of the breakthrough curve, a borosilicate glass column with an inner diameter of 1.5 cm and a total height of 20 cm (adjustable) was used. The column was packed with 5.0 g of wet KG-GO-CA hydrogel beads, and the bed height was set to 6.0 cm. The column was partially filled with water during packing to prevent the hydrogel from drying out, and compaction was achieved naturally by gravity. Before starting the adsorption tests, water was pumped through the system for approximately 25 minutes to remove air bubbles and ensure there were no leaks**.** The fixed bed experiment was conducted at an average flow rate of 2.0 mL/min, with a feed concentration of 20 mg/L for AB 113 dye. To regenerate the column, the system was fed with 0.10 M NaOH. The breakthrough curve facilitated the estimation of breakthrough time (t_{BR}), exhaustion time (t_{EX}), stoichiometric time (t_{st}), and adsorption capacity (q_{eq}). The breakthrough time represented the point at which the concentration ratio C_t/C_0 reached 0.05, while the exhaustion time indicated when the ratio C_t/C_0 reached 0.95 (de Araujo et al., 2022). The stoichiometric time (t_{st}) was determined using Eq. (5.8). The Thomas model described the movement of solute through a liquid film to the adsorbent surface during adsorption (Eq. 5.9). It explained how solute molecules diffused through the liquid film and got trapped on the adsorbent's surface, forming an adsorbed layer. The removal efficiency was calculated using Eq. (5.10).

$$t_{st} = \int_0^{\infty} \left(1 - \frac{C_t}{C_{\infty}}\right) dt \tag{5.8}$$

$$\frac{C_t}{C_0} = \frac{1}{1+\exp\left(\frac{K_{Th}\, q_e\, m}{Q} - K_{Th} C_0\, t\right)} \tag{5.9}$$

$$\%\ \text{Removal} = \frac{\int_0^{\infty} \left(1 - \frac{C_t}{C_{\infty}}\right) dt}{t_f} \times 100 \tag{5.10}$$

where C_∞ represents the equilibrium concentration, and $C_0 = C_\infty$, Q is the constant inlet flow rate, V is the volume of the column, m is the mass of adsorbent in the fixed-bed column, K_{Th} = Rate constant of the Thomas model, and t_f is the overall time in which C_t approaches C_∞.

5.3.9 Assessment of residual toxicity

Bacterial cell viability reflects the functional state of live bacteria in a given environment. It indicates whether bacterial cells are active, metabolically functional, and capable of carrying out their normal biological processes. Three bacterial strains viz. *E. coli*, *Bacillus tequilensis*, and *Pseudomonas aeruginosa* were used for the toxicity assessment of AB 113 (100 mg/L). Bacterial cultures were allowed to grow overnight in nutrient broth, and the log phase (exponential phase) of the culture was extracted through the centrifuge (REMI CENTRIFUGE, RM- 12C BL, 5000 rpm, 15 min). Phosphate buffered saline was used for the washing of obtained pellets and ensured that there should be no residue of the nutrient. The pellets having a cell concentration of 2×10^6 CFU/mL, were used to prepare bacterial cultures in nutrient broth for toxicity analysis. AB 113 (100 mg/L) and KG-GO-CA hydrogel treated AB 113 were exposed to the three bacterial species culture medium and subjected to incubation for 24 h at 35 ± 2 °C. Using a conventional plate count test cellular viability of the control and treated bacteria was calculated after 24 hours (Ravikumar et al., 2018). The viability of the treated cells was estimated using the control as a reference.

5.3 Results and Discussion

5.3.1 Characterization

5.3.1.1 Zeta potential and Particle size distribution

The size and stability of synthesized GO were investigated by analyzing the particle size distribution and zeta potential. The results revealed that the average particle size of GO was 1061 nm (**Figure 5.5a**), with a narrow particle size distribution as indicated by the low

Polydispersity index (PdI) value of 0.168. This suggested that GO had a uniform particle size distribution in aqueous media when dispersed in distilled water, which had a refractive index of 1.330, a viscosity of 0.8872 cP, and a dielectric constant of 78.5.

The zeta potential and zeta deviation of GO were found to be -31 mV and 5.02 mV, respectively (**Figure 5.5b**). The negative zeta potential indicated that the GO particles had a high surface charge, which contributed to the stability of the formed colloidal solution after complete dispersion. The low zeta deviation suggested that the GO particles had a relatively homogeneous surface charge distribution.

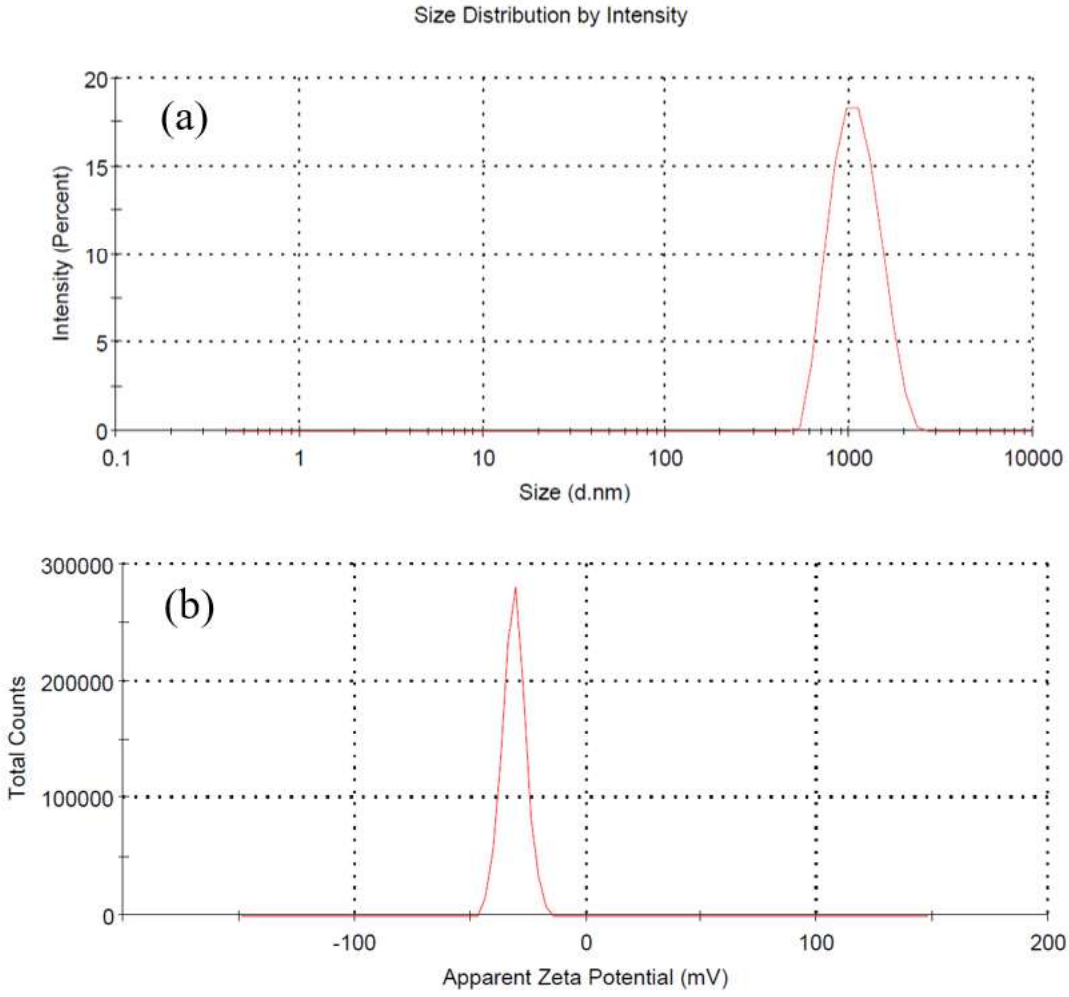

Figure 5.5. A comprehensive view of GO nanoparticles: (a) assessment of particle size distribution and (b) evaluation of zeta potential distribution

5.3.1.2 FTIR Spectral Analysis

The FTIR analysis of GO and KG-GO-CA hydrogel beads was performed to elucidate the functional groups. The strong broad peak observed at 3390 cm^{-1} in the GO spectrum indicated the presence of hydroxyl groups (–OH) and formyl (C-OH) groups at the edges of GO nanosheets (**Figure 5.6**). The peaks at 2889, 1709, and 1621 cm^{-1} corresponded to the medium C-H stretching of alkane, strong stretching of carboxyl groups (–C=O), and alkene (C=C) of the sp^2 hybridized carbon chains of GO, respectively (Lentz et al., 2022). The epoxy bridges (C-O-C) and pairwise carboxyl groups (-COOH) were attributed to the wavenumbers of 1173 and 1062 cm^{-1}, respectively.

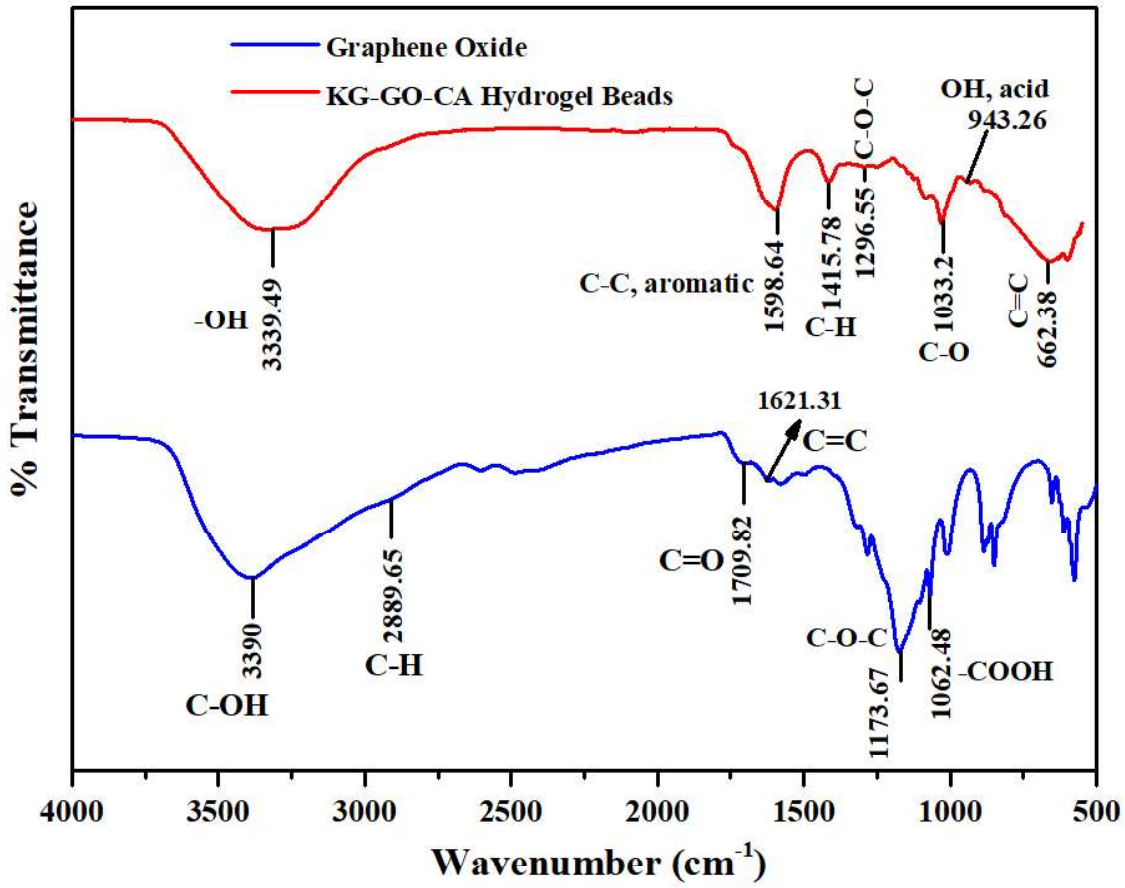

Figure 5.6. Distinctive FTIR spectra of Graphene Oxide and *Klebsiella grimontii* cell entrapped Graphene oxide-Calcium alginate (KG-GO-CA) hydrogel beads, showcasing the successful encapsulation of GO and bacterial cell in the hydrogel matrix

In the KG-GO-CA hydrogel beads, a strong broad stretching at a wavenumber of 3339 cm^{-1} indicated the presence of hydroxyl group (-OH) in the alginate matrix (**Figure 5.6**). This can be attributed to the intermolecular interactions between GO and SA, which were caused by hydrogen bonds (Jiao et al., 2016). This confirmed that gelation had occurred. The sharp peaks observed at 1598, 1415, and 1033 cm^{-1} were indicative of the presence of medium C-C stretching of an aromatic ring, medium C-H bending of alkane, and strong C-O stretching of epoxy groups, respectively. The slightly medium peaks at wavenumbers of 1296 cm^{-1} and 943 cm^{-1} were attributed to the presence of epoxy bridges (C-O-C) and the medium bending of carboxylic acid (-OH), respectively. The strong bending of alkene (-C=C) present in the GO-CA polymer network was reasonably due to the sharp peak observed at 662 cm^{-1}. The addition of HCl aided in the rapid release of CO_2 gas to promote pore formation and cross-link alginate with Ca^{2+} ions simultaneously. This resulted in the formation of GO-CA hydrogel beads with improved properties.

5.3.1.3 High-Resolution X-Ray Diffraction (HR-XRD) Spectra

This study confirmed the interaction between GO and the *Klebsiella grimontii* cell-entrapped alginate-based polymer matrix through HR-XRD spectra. The continuous reduction of GO by bacteria led to the formation of reduced Graphene Oxide (rGO). The π-π interaction between the adjacent layers of GO resulted in the squeezing of water molecules and getting stacked (Shen et al., 2018). In the XRD spectra of GO, a characteristic major peak at 11.32˚ (0 0 1) and a minor peak at 42.5˚ (1 1 1) was observed (**Figure 5.7**). This major peak at 11.32˚ (0 0 1) was known to correspond to the expansion of the (0 0 2) plane from graphite due to the insertion of oxygenated functional groups. The interaction of bacterial species and GO led to the formation of the peak at 24.3˚ (0 0 2), which was reasonably similar to the characteristic peak of rGO. The characteristic peak of GO disappeared during the formation of the polymer matrix (GO-

CA hydrogel beads) with cross-linking of Ca^{2+} ions and the cell entrapment of *Klebsiella grimontii*.

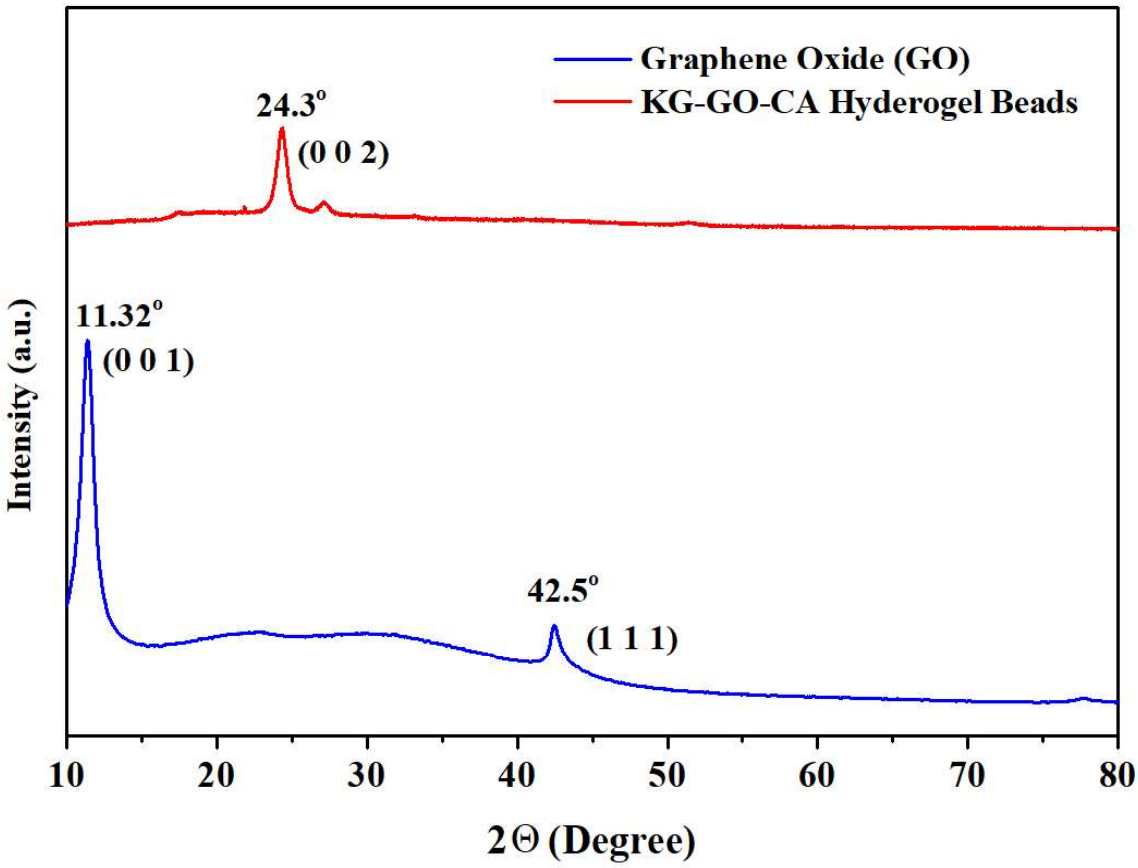

Figure 5.7. Revealing the Crystallographic Insights: XRD Analysis of Graphene Oxide and *Klebsiella grimontii* cell entrapped Graphene Oxide-Calcium Alginate (KG-GO-CA) hydrogel beads

The peak at 11.32˚ disappeared, indicating that GO was mixed with an alginate polymer matrix. It was due to the interactions between the hydroxyl and carboxyl groups of GO and the alginate polymer matrix. The distance between the layers of GO and KG-GO-CA hydrogel beads called interplanar spacing (d), was measured to be 0.78 nm and 0.37 nm, respectively. The smaller interplanar spacing (0.37 nm) in KG-GO-CA hydrogel beads was due to strong interactions between the GO sheets and the alginate polymer matrix (Sun and Fugetsu, 2014). The interactions between the components improved their uniformity and made them mix well,

resulting in the formation of the desired hydrogel beads. This happened because the GO sheets were evenly distributed and well spread out within the CA polymer matrix.

5.3.1.4 Thermogravimetric Analysis (TGA)

The thermal stability of GO and KG-GO-CA hydrogel beads was investigated using TGA. The TGA curves of both samples exhibited different weight loss regions, indicating their distinct thermal stability characteristics. The first weight loss (12.25%) of GO occurred between 25 °C to 135 °C, which was attributed to the volatilization of water due to the presence of hydrophilic groups in GO (**Figure 5.8**). The second weight loss (4.52%) within the temperature range of 135 °C to 254 °C was due to the decomposition of oxygen groups, including C=O, C-O-C (epoxy group), and C-O (Lin et al., 2020). The third weight loss (23.42%) and final weight loss (9.32%) occurred between 254 °C to 383 °C and 383 °C to 600 °C, respectively, due to the breakdown of carbon and carbon-skeleton in GO, particularly the carbonization of sp^2 and sp^3 hybrid carbon atoms (Lin et al., 2020).

In contrast, the thermal degradation of KG-GO-CA hydrogel beads was a two-stage process, with the first major weight loss (63.60%) occurring within the temperature range of 24 °C to 130 °C (**Figure 5.8**). This weight loss was attributed to the breakdown of chains, fragments, and monolayers of alginate, followed by the decomposition of GO (Sun and Fugetsu, 2014). Since GO enhanced porosity, more water might be introduced by hydrogen bonding, creating additional active sites. Moreover, GO possessed a basal plane that contained diverse oxygen-containing functional groups and was susceptible to changes in thermal stability. Therefore, additional weight loss was hindered, and only 11.86% and 10.41% weight loss occurred with corresponding temperature ranges of 130 °C to 178 °C and 178 °C to 600 °C, respectively.

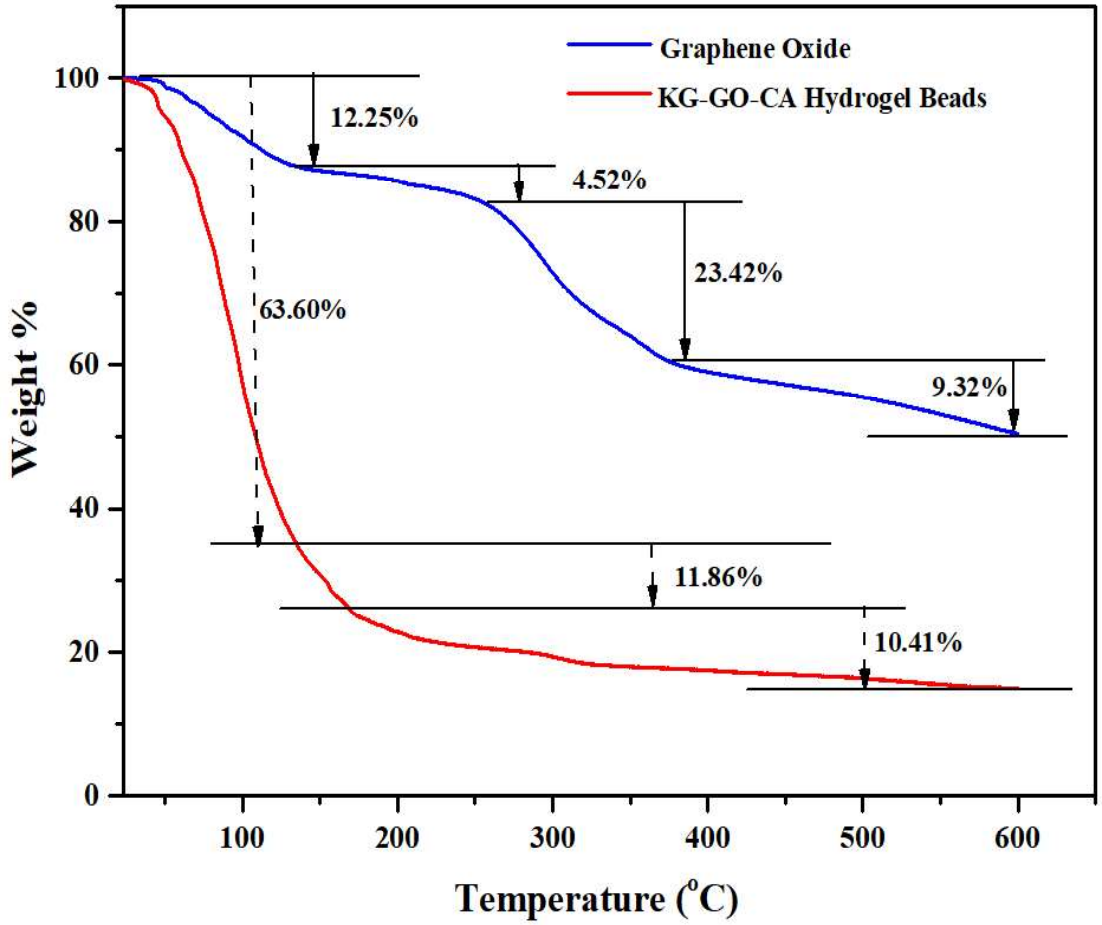

Figure 5.8. TGA Analysis: An Insight into the Thermal Behavior of GO and KG-GO-CA hydrogel beads

5.3.1.5 Surface area and pore size distribution analysis

The N_2 adsorption-desorption isotherms of GO and KG-GO-CA hydrogel beads exhibited a type H4 and H3 hysteresis loop, respectively, and were categorized as type IV isotherms (**Figure 5.9a**). Type H3 hysteresis loop indicated the presence of silt-shaped and parallel plate-shaped (groove) pores, while type H4 resembled the formation of slit/wedge-shaped pores. These pores can be attributed to the unique structure and morphology of GO and KG-GO-CA hydrogel beads.

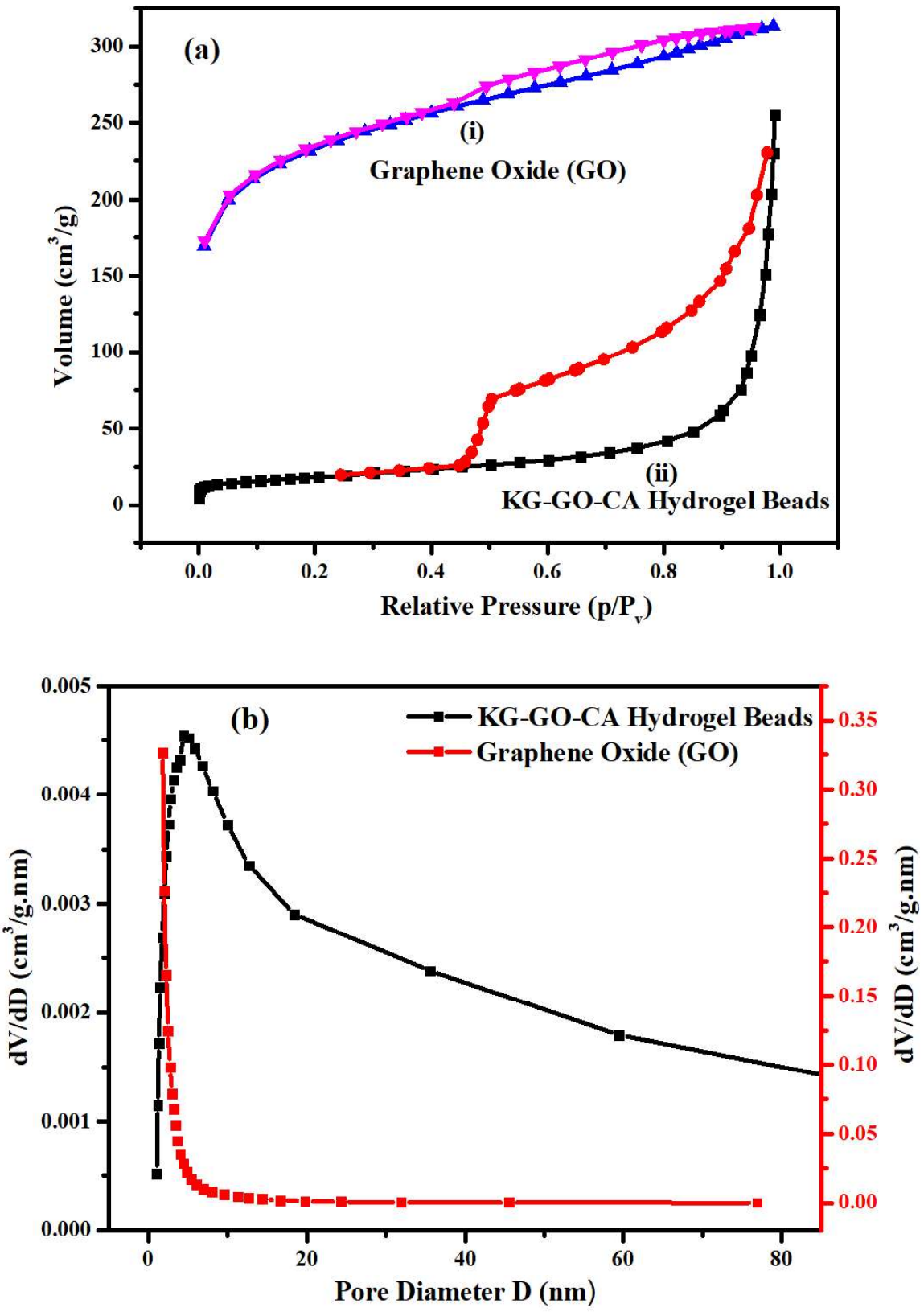

Figure 5.9. Characterizing the pore structure of GO and KG-GO-CA hydrogel beads: insights from (a) N_2 adsorption-desorption isotherm and (b) BJH pore size distribution

The average pore diameter of GO and KG-GO-CA hydrogel beads were 2.87 and 24.542 nm, respectively (**Figure 5.9b**). The average pore diameters of both samples were within the mesoporous range (2-50 nm) (Zhang et al., 2016). The specific surface area (BET surface area) of GO and KG-GO-CA hydrogel beads were determined to be 770.69 m^2/g and 64.18 m^2/g, respectively. This suggested that GO had a significantly higher specific surface area than KG-GO-CA hydrogel beads. However, the incorporation of the calcium alginate matrix resulted in the formation of larger pores in KG-GO-CA hydrogel beads, which could have advantages for the biosorption of dyes.

5.3.1.6 Scanning Electron Microscopy (SEM) Analysis

The surface morphologies of synthesized GO and KG-GO-CA hydrogel beads were investigated using SEM. The SEM images revealed differences between the two samples (**Figure 5.10**). Interestingly, cross-linking with Ca^{2+} ions, along with entrapped *Klebsiella grimontii* cells, was responsible for the porous nature of KG-GO-CA hydrogel beads. This addition of GO could improve the porous nature of the hydrogel beads, which was crucial for their biosorption applications. Furthermore, some buckling in the surface of KG-GO-CA hydrogel beads was observed after the addition of GO, indicating a satisfactory interaction between CA and GO. The amphipathic GO sheets were crucial for the creation of GO-CA hydrogels, as reported in previous studies (Jiao et al., 2016). Optical images and size distribution analysis of KG-GO-CA hydrogel beads were incorporated, demonstrating the unique inter-connected adjacent layer formation on the surface (**Figure 5.11, 5.12**).

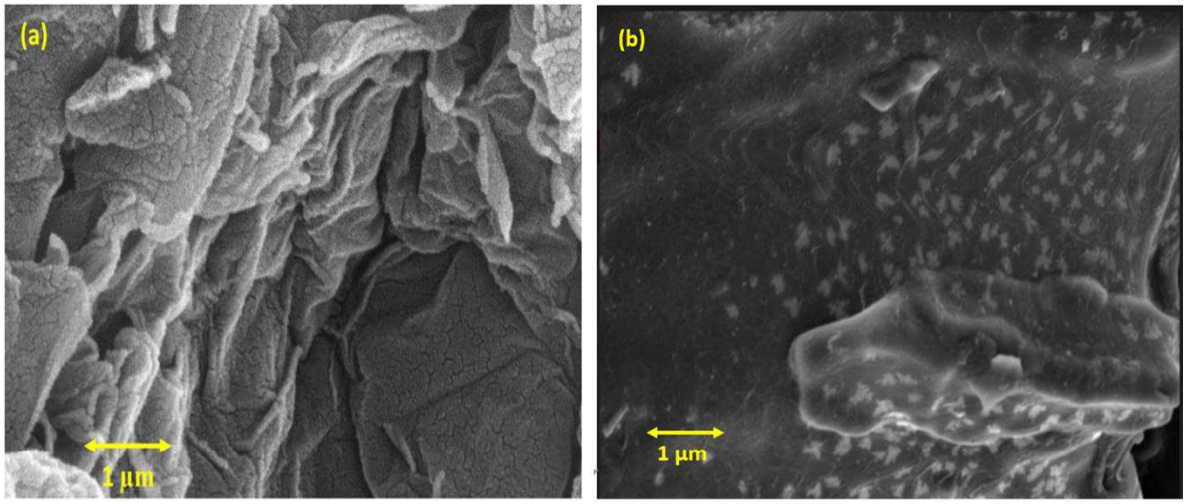

Figure 5.10. SEM images of (a) Graphene Oxide (GO) and (b) KG-GO-CA hydrogel beads reveal the porous, three-dimensional structure of these materials. The scale bar is 1 µm

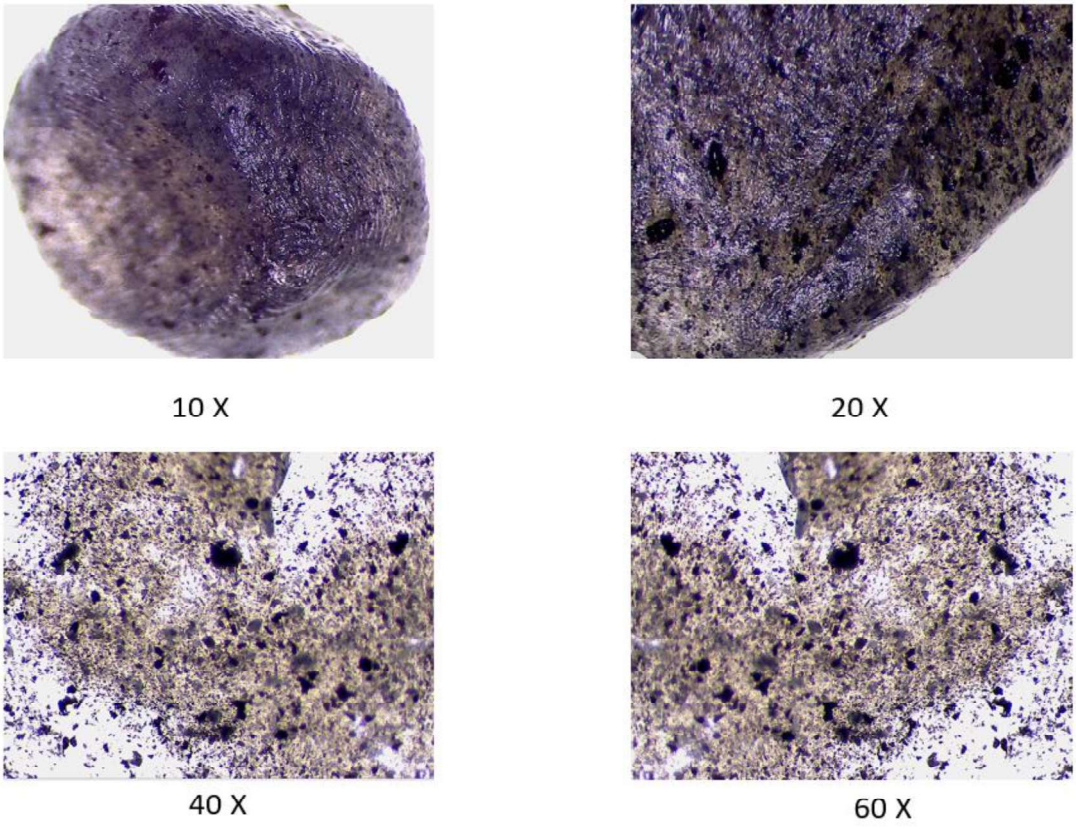

Figure 5.11. Optical Microscope images of KG-GO-CA hydrogel at various magnifications

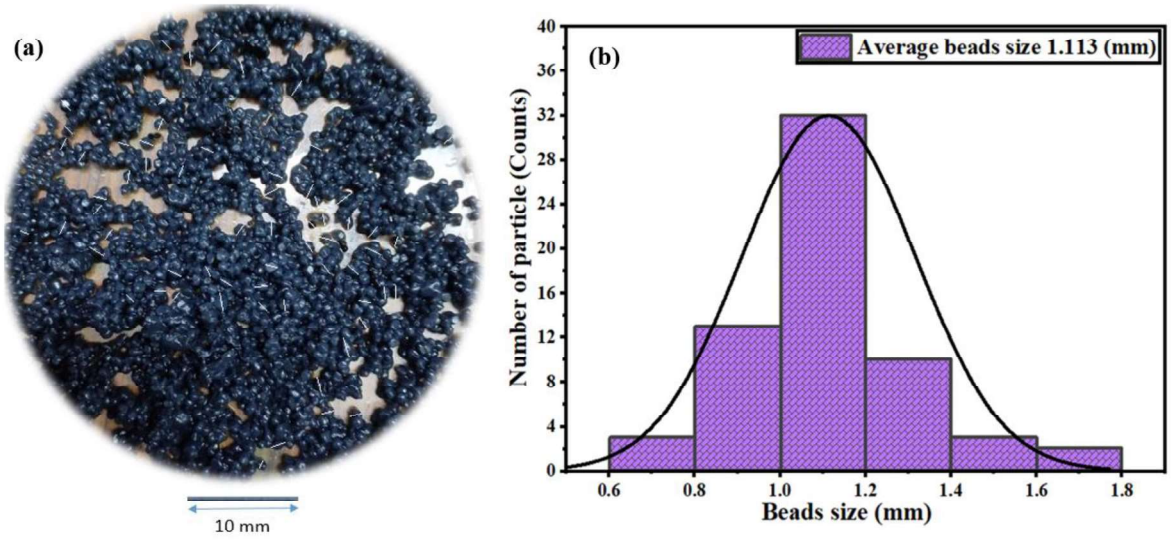

Figure 5.12. (a) An approximate size distribution of KG-GO-CA hydrogel beads and (b) Histogram size distribution using ImageJ image analyzer

5.3.2 Expansion and Fluidization Behavior of FBBR

An experimental investigation was carried out to examine the fluidization behavior and the resulting expansion of bed height by varying the superficial velocity of air. The bed height increased steadily with the increase in the superficial velocity. When the superficial velocity reached 0.15 mm/s, the bed height expanded by a factor of 1.6, and a further increase in velocity caused the bed to expand even more (**Figure 5.13**). This implied that the minimum fluidization velocity for KG-GO-CA hydrogel beads was 0.15 mm/s. Moreover, the bed expansion exhibited a linear relationship with increasing air superficial velocity. At 0.2 mm/s, the bed expanded 2.12-fold, and at 0.32 mm/s, it expanded almost 3-fold. When the air was introduced into the FBBR in an upward direction, the KG-GO-CA hydrogel beads started moving from the bottom to the top layers. The movement was more pronounced in the central region of the column, where a bottom-to-top mixing pattern was observed. As the bed became progressively fluidized, the beads moved downward along the wall due to drag, while the expansion level

was maintained. Nevertheless, the system demonstrated stable and coherent fluidization of KG-GO-CA hydrogel beads.

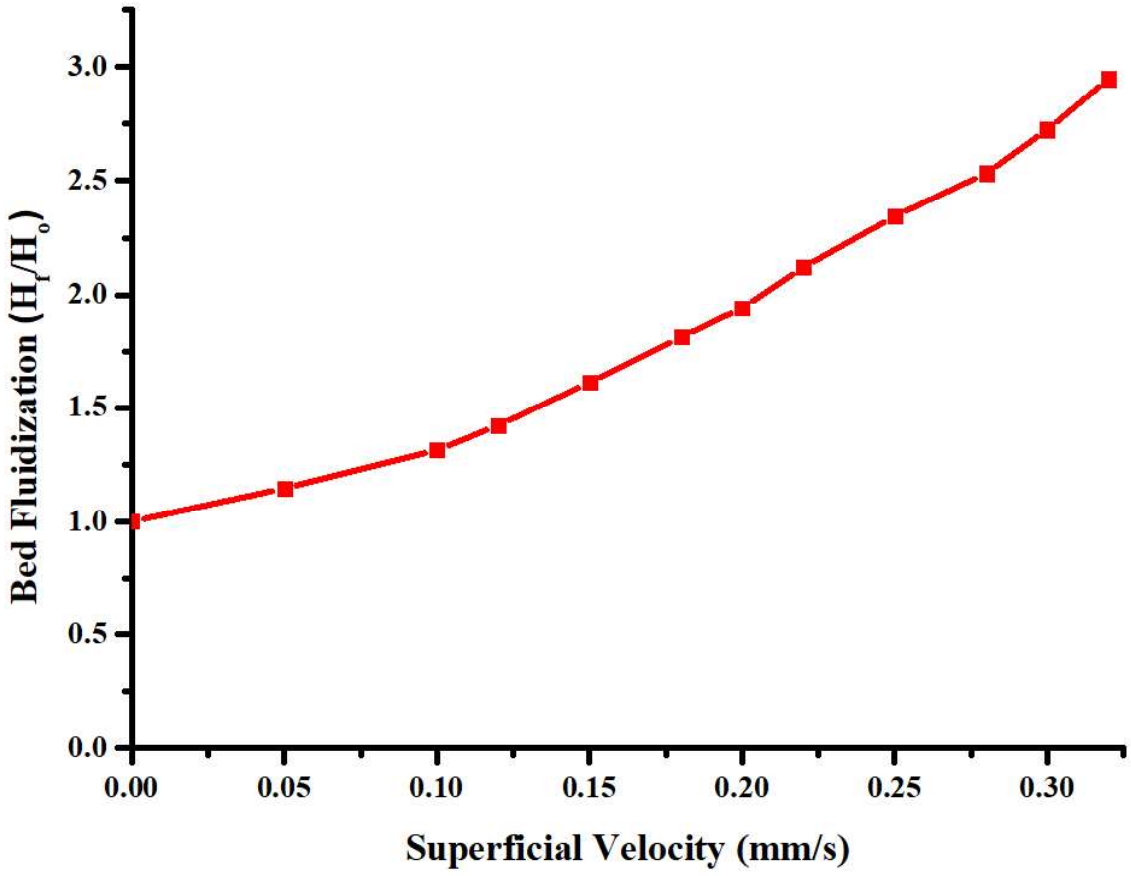

Figure 5.13. An in-depth look at the Fluidization characteristics of *Klebsiella grimontii* cell-entrapped GO-CA hydrogel beads in a FBBR system: Understanding bed height expansion (H_f) and its relationship to initial bed height (H_o) at varying air superficial velocities

5.3.3 OUR and DO consumption by KG-GO-CA hydrogel beads

The GO-CA hydrogel beads with entrapped bacterial cells of *Klebsiella grimontii* consumed oxygen and AB 113 (**Figure 5.14**). The biodegradation continued when it was determined that the bacteria were alive and in their active life cycle. The oxygen saturation was 7.21 mg/L. The DO concentration needed to be kept above 10% of saturation to prevent microorganisms from perishing through lack of oxygen (Garcia-Ochoa et al., 2010). Consequently, DO concentration

was kept above 7.21 mg/L during the biodegradation through aeration. This study elucidated the OUR as a measure associated with *Klebsiella grimontii* activity to degrade the AB 113 in the wastewater; since the maximum DO concentration was constrained by the poor solubility of oxygen. After 12 hours, the AB 113 wastewater sample containing the KG-GO-CA hydrogel beads exhibited complete DO depletion due to the microbes' oxygen consumption (**Figure 5.14**). The experimental findings of both DO and OUR were fitted through the nonlinear polynomial curve fitting. The initial OUR was 0.352 mg/L.h. As the biodegradation further proceeded, the OUR increased, and after 4 h, the OUR reached a maximum of 0.968 mg/L.h (**Figure. 5.14**). Since the oxygen was continuously consumed by the bacterial cell culture, the DO level was decreased. Thus, after 4 h, the OUR decreased from 0.968 mg/L.h to 0.12 mg/L.h in12 h. OUR and DO consumption were somehow directly dependent on the amount of biomass produced (Bustos-Terrones et al., 2022).

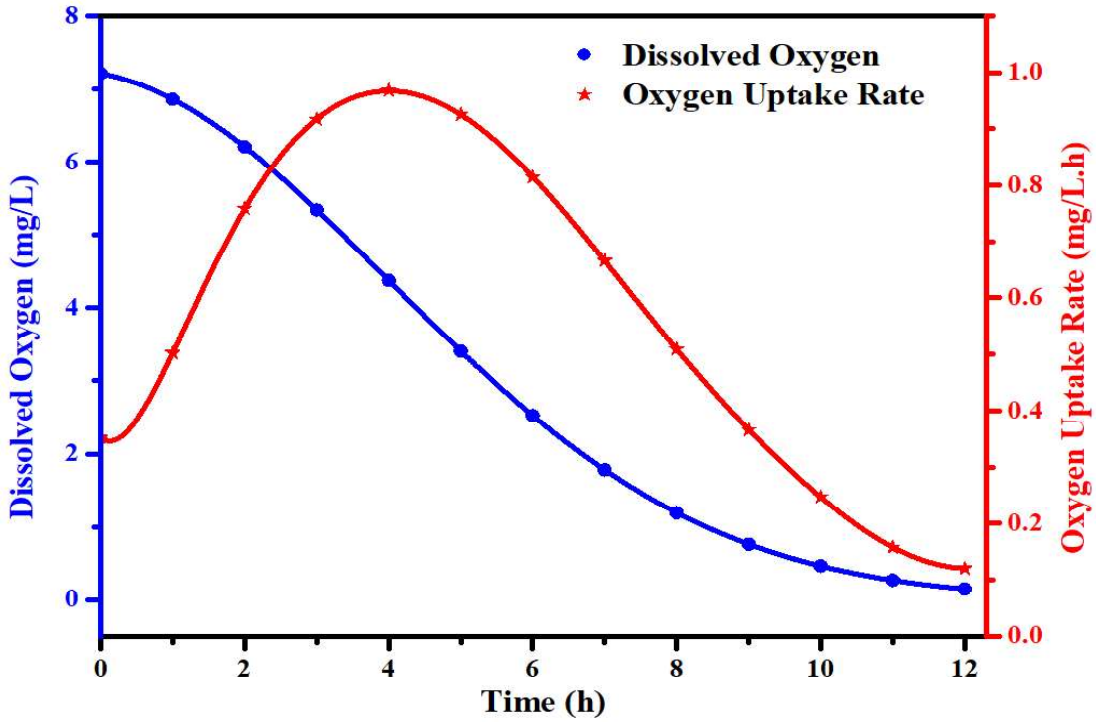

Figure 5.14. A typical variation of Dissolved oxygen (DO) and Oxygen uptake rate (OUR) of *Klebsiella grimontii* during the biodegradation of AB 113

5.3.4 Biosorption Performance evaluation of Acid Blue 113 dye in a Continuous FBBR

The removal efficiency of AB 113 was dependent on the inlet flow rate. The preliminary batch experiment suggested that the optimum pH and AB 113 concentration were 7.0 and 50 mg/L, respectively. The performance of continuous FBBR was assessed in terms of RE and EC under optimum conditions at varying flow rates (20- 80 mL/h) and inlet shock loading rates (ISLR) (25- 100 mg/L.day). The continuous FBBR was initially operated with an ISLR of 25 mg/L.day with an inlet flow rate of 20 mL/h. The EC and RE began to increase exponentially and at the end of the 15^{th} day under equilibrium, the FBBR reached 23.8 mg/L.day EC and 94.6% RE, respectively (**Figure 5.15a**). The overall performance of the continuous FBBR biosorption process was presented in **Table 5.1**. A sharp declination in the RE was observed as the flow rate steadily increased to 40 mL/h with a corresponding ISLR of 50 mg/L.day. The RE steadily recovered, after the 30^{th} day, the EC and RE were 44.6 mg/L.day and 90.4%, respectively. Meanwhile, there was an increment in the EC was observed. Furthermore, on the 30^{th} day, the flow rate was again step changed and FBBR was allowed to operate with a 60 mL/h flow rate and 75 mg/L.day ISLR, respectively. The RE sharply decreased to 70% on the 34^{th} day, thereafter as the EC steadily reached 57.1 mg/L.day at the end of the 45^{th} day, the RE was further recovered and reached 86.1%. At the flow rate of 80 mL/h, further, the RE sharply decreased and attained a steady state at 70.8% RE and the maximum EC of 62.4 mg/L.day.

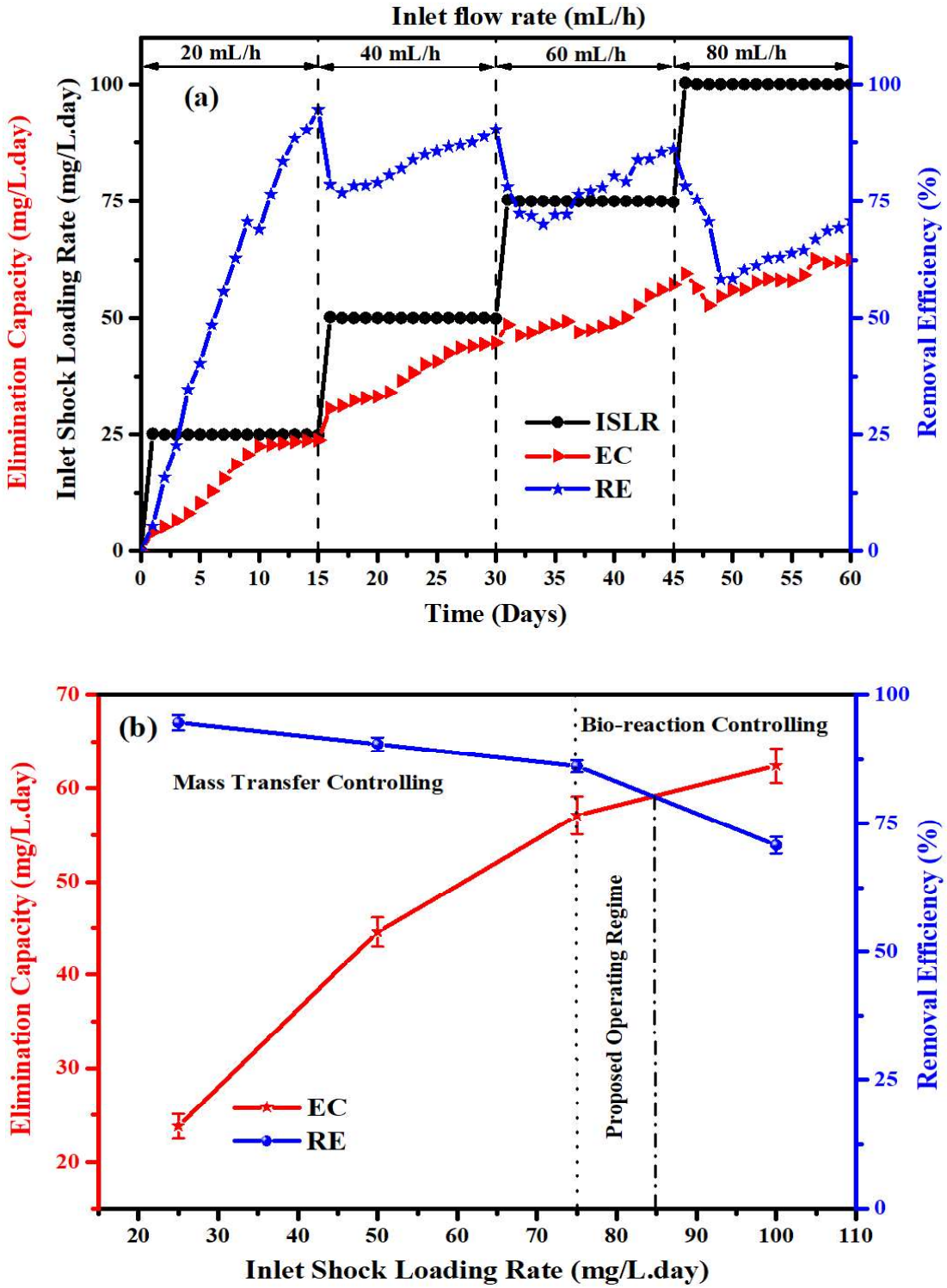

Figure 5.15. Biosorption process performance of a continuous FBBR under optimum conditions: (a) Impact of inlet shock loading rate on AB 113 elimination capacity and removal efficiency; (b) Typical correlation between bio-reaction and mass transfer controlling regime observed with variations in inlet shock loading rate of AB 113

Table 5.1 Performance of continuous Fluidized Bed Bioreactor for biosorption of Acid Blue 113 dye.

Inlet Flow rate (mL/h)	Bioreactor process time (day)	Inlet Shock Loading Rates (mg/L.day)	AB 113 Removal Efficiency (%)	Elimination Capacity (mg/L.day)
20	1-15	25	94.6	23.8
40	15-30	50	90.4	44.6
60	30-45	75	86.1	57.1
80	45-60	100	70.8	62.4

AB 113 RE was decreased from 94.6% to 70.8% as the inlet flow rate was increased from 20 to 80 mL/h. The above fact could be attributed to the shorter hydraulic retention time (HRT) of AB 113 inside the FBBR as the inlet flow rate was increased (Sonwani et al., 2020). Another reason could have been mass transfer limitations, which occurred when the rate of dye transfer from the bulk solution to the surface of the KG-GO-CA hydrogel beads (biosorbent) was slower than the rate of diffusion of the dye within the biosorbent. This might have resulted in a lower removal efficiency, especially at higher flow rates. A similar kind of work had been performed for the biodegradation of malachite green dye using the Calcium alginate beads immobilized with *Bacillus cereus* and proposed that at a high inlet flow rate, the RE declined (Nath et al., 2016).

The present study illustrated the variation of EC and RE in response to increasing ISLR of AB 113, as depicted in **Figure 5.15b**. The results revealed that RE exhibited a slight decrease upon increasing ISLR to 75 mg/L.day, followed by a sharp decline. In contrast, EC displayed a linear correlation with ISLR up to 75 mg/L.day, followed by a non-linear increase. The highest EC value of 62.4 mg/L.day was obtained at an ISLR of 100 mg/L.day. The performance of the bioreactor process exhibited a decline at a high inlet flow rate, which can be attributed to the

onset of simultaneous rate-controlling mechanisms (Mohanty and Kumar, 2021). The biodegradation of AB 113 was examined at various ISLRs to determine the rate-controlling mechanism, which was found to be influenced by both mass transfer and bio-reaction. At low ISLR, the diffusion of dye through the biosorbent's outer layer was slow, resulting in a deficiency of substrate (AB 113) in the inner regime where microbes were immobilized, indicating a mass transfer control mechanism (Kathiravan et al., 2014). Conversely, at high ISLR, the diffusional flux of dye increased, resulting in a shift in the biodegradation rate-controlling mechanism from mass transfer control to bio-reaction control (Geed et al., 2017; Sonwani et al., 2020; Yadav et al., 2014).

In bioreactors, the mechanism controlling the process can switch from mass transfer control to bio-reaction control depending on the lower limit of ISLR. The point where this switch occurred was of practical importance, while the point where the EC intersected with the RE could be considered an extreme limit (Geed et al., 2017). The present finding determined the optimal range of ISLR for the effective degradation of Acid Blue 113 dye. The results indicated an inlet loading rate between 75 and 85 mg/L.day led to the most efficient degradation of the dye.

5.3.5 Reusability of KG-GO-CA hydrogel beads

The ability of an adsorbent to be regenerated was crucial for wastewater treatment. Adsorption/desorption cycles were used to assess the KG-GO-CA and CA hydrogel's reusability. The comparative reusability study of KG-GO-CA and CA hydrogel beads revealed that KG-GO-CA had more dye removal efficiency even after the end of the 12^{th} cycle (**Figure 5.16**). Pure CA hydrogel beads lost their adsorption capacity (66.8 ± 1.3% dye removal), whereas KG-GO-CA hydrogel beads exhibited 70.6 ± 2.5% dye removal efficiency after successively reused at the end of 12^{th} cycle. KG-GO-CA hydrogel beads exhibited more dye

adsorption capacity compared to the CA hydrogel beads which could be due to the presence of oxygen-containing functional groups in the basal plane of GO. However, both were cross-linked with Ca^{2+} ions. It indicated that the polymer network in GO-CA effectively adhered GO nanosheets and AB 113, suppressed the swelling of alginate, facilitated regeneration, and remained stable. After 12 adsorption/desorption cycles, the adsorption capacities of AB 113 for GO-CA and CA hydrogel beads were 73.2% and 70.9% of their original adsorption capacity, respectively. Therefore, KG-GO-CA hydrogel beads had shown improved adsorption efficiency compared with CA hydrogel beads. A similar study was carried out for the rhodamine B (RB) dye using SA-rGO-4 and achieved 90% of the original adsorption capacity after 10 adsorption/desorption cycles (Xiao et al., 2020).

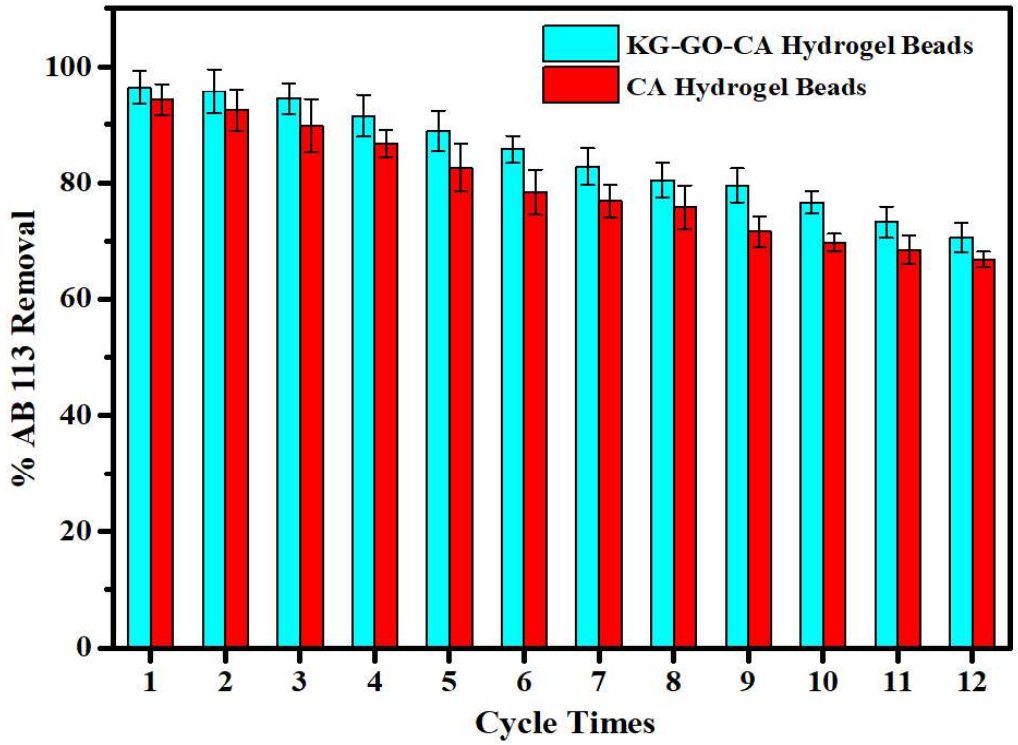

Figure 5.16. A successive adsorption/desorption comparison study of AB 113 using KG-GO-CA and CA hydrogel beads (AB 113 = 50 mg/L; Temperature = 30 ± 2 °C; Bacterial cell concentration = 2×10^6 CFU/mL) (Error bars depicted the standard deviation of triplicate study)

5.3.6 Adsorption isotherm of KG-GO-CA hydrogel beads

KG-GO-CA hydrogel beads had been used for the batch adsorption study of AB 113. It was determined that the adsorption capacity tended to rise with AB 113 equilibrium concentrations before gradually reaching the plateau maximum (**Figure 5.17**). Their adsorption characteristics were determined using non-linear Langmuir (Eq. 5.6) and Freundlich (Eq. 5.7) isotherm models. It can be observed from the isotherm data that the Langmuir model was more effective than the Freundlich model in describing the adsorption process, as evidenced by its higher regression coefficient (R^2 = 0.98724). The model parameters of both isotherms were calculated and illustrated in **Table 5.2**.

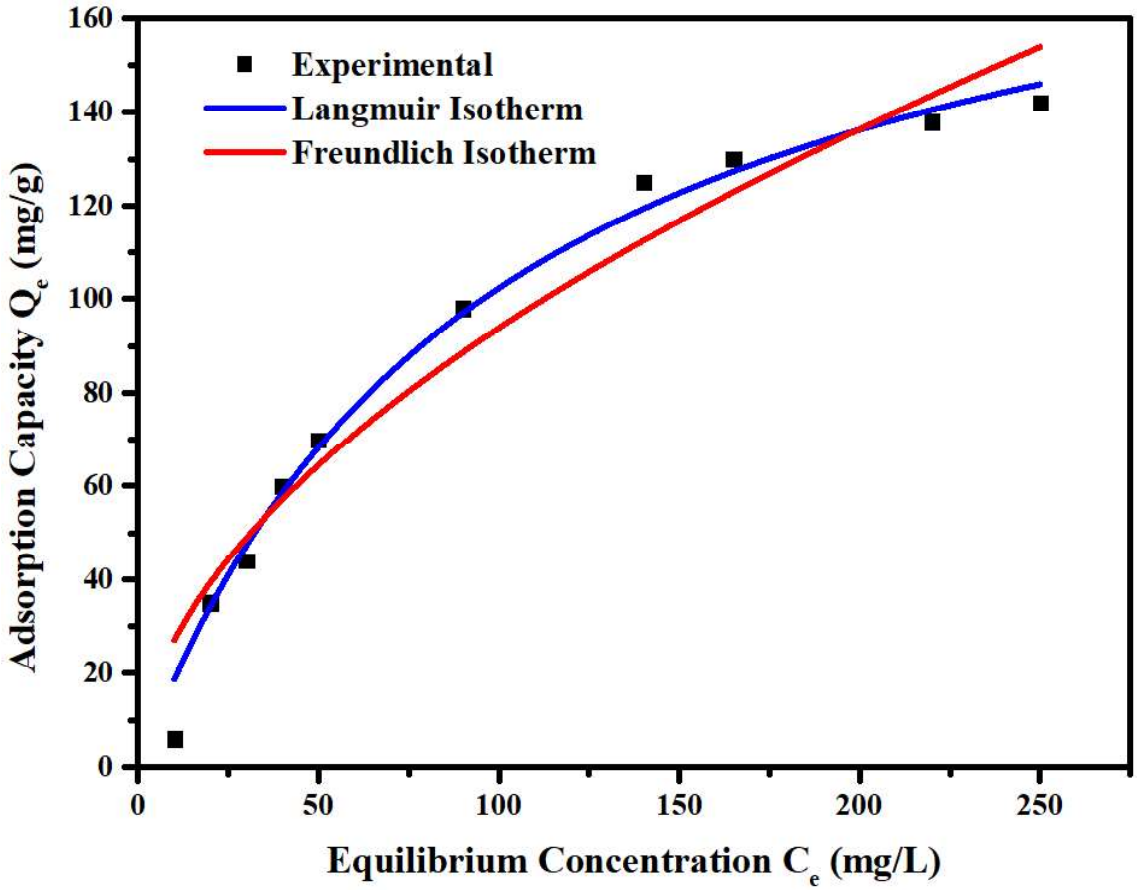

Figure 5.17. Evaluating the suitability of Langmuir and Freundlich isotherm models to describe the adsorption of AB 113 onto KG-GO-CA hydrogel beads at 27 °C, pH 7 ± 0.5, and 12 h duration

Table 5.2 Langmuir and Freundlich isotherm model parameters.

S.N.	Langmuir Isotherm parameters	Freundlich Isotherm parameters
1.	Q_m = 203.83 mg/g	K_f = 7.805 L/g
2.	K_i = 0.0101 L/g	n = 1.852
3.	R^2 = 0.98724	R^2 = 0.94723

The above finding supported the hypothesis that the KG-GO-CA hydrogel beads have a homogeneous surface and that the AB 113 dye adhered to the adsorbent uniformly.

5.3.7 Fixed-Bed Adsorption

The results of the Breakthrough curve experiments were analyzed using the Thomas model, which involved fitting the experimental data to the model (**Figure 5.18**). Based on these fittings, important parameters such as the breakthrough time, exhaustion time, and stoichiometric time were determined (**Table 5.3**).

Table 5.3 Experimental findings of various parameters using Breakthrough curve.

S.N.	Parameters	Results
1.	t_{BR} (min)	257.3
2.	t_{EX} (min)	706.51
3.	t_f (min)	1000
4.	t_{st} (min)	457.84
5.	% Removal	45.78
6.	q_e (mg/g)	7.276
7.	K_{Th} (mL/min.mg)	0.35

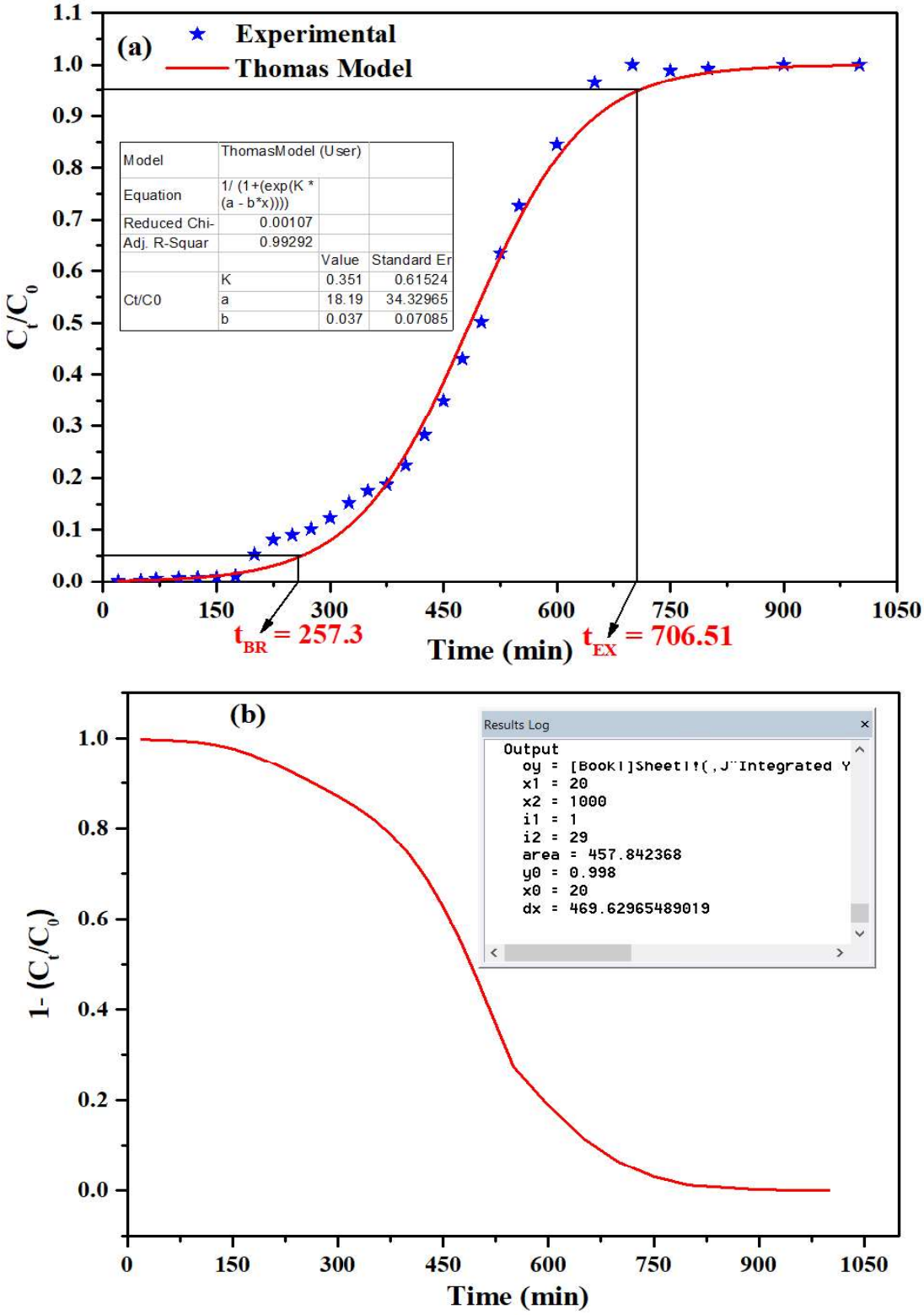

Figure 5.18. Breakthrough Curve for adsorption of AB 113 onto KG-GO-CA hydrogel beads (a) Experimental data fitted with Thomas model, (b) Stoichiometric time and % Removal determination (T = 27 °C; pH = 7)

The breakthrough curve presented a characteristic symmetric S-shape, with the basic Fuchsin curve showing the most pronounced S-shape. Dispersion effects were observed in this breakthrough curve and occurred due to various factors, including axial dispersion, mass transfer resistances, non-ideal packing of the column, and uneven fluid distribution throughout the column (de Araujo et al., 2022). These dispersion effects led to variations in the AB 113 movement and distribution within the column, influencing the shape and behavior of the breakthrough curve during the adsorption process.

5.3.8 Residual Toxicity of Acid Blue 113 and KG-GO-CA hydrogel beads treated AB 113

The residual toxicity assessments are crucial in ensuring the safety of industrial effluents, especially those containing potentially harmful complex dyes like Acid Blue 113. In this study, the cell viability of three bacterial strains (*Bacillus tequilensis*, *E. coli*, and *Pseudomonas aeruginosa*) had examined to assess the residual toxicity of AB 113. The results demonstrated that the treatment with these hydrogel beads significantly increased the cell viability of all three bacterial strains. Specifically, the relative cell viability of treated AB 113 increased by 51.45%, 51.76%, and 65.79% for *Bacillus tequilensis*, *E. coli*, and *Pseudomonas aeruginosa*, respectively (**Figure 5.19**). These findings suggested that the application of KG-GO-CA hydrogel beads could be a promising solution for reducing the effective toxicity of AB 113, thus minimizing its impact on the environment and living organisms. Furthermore, the use of KG-GO-CA hydrogel beads represented a promising approach to address the residual toxicity of AB 113. It might have important implications for the development of more sustainable and eco-friendly technologies for contaminants remediation.

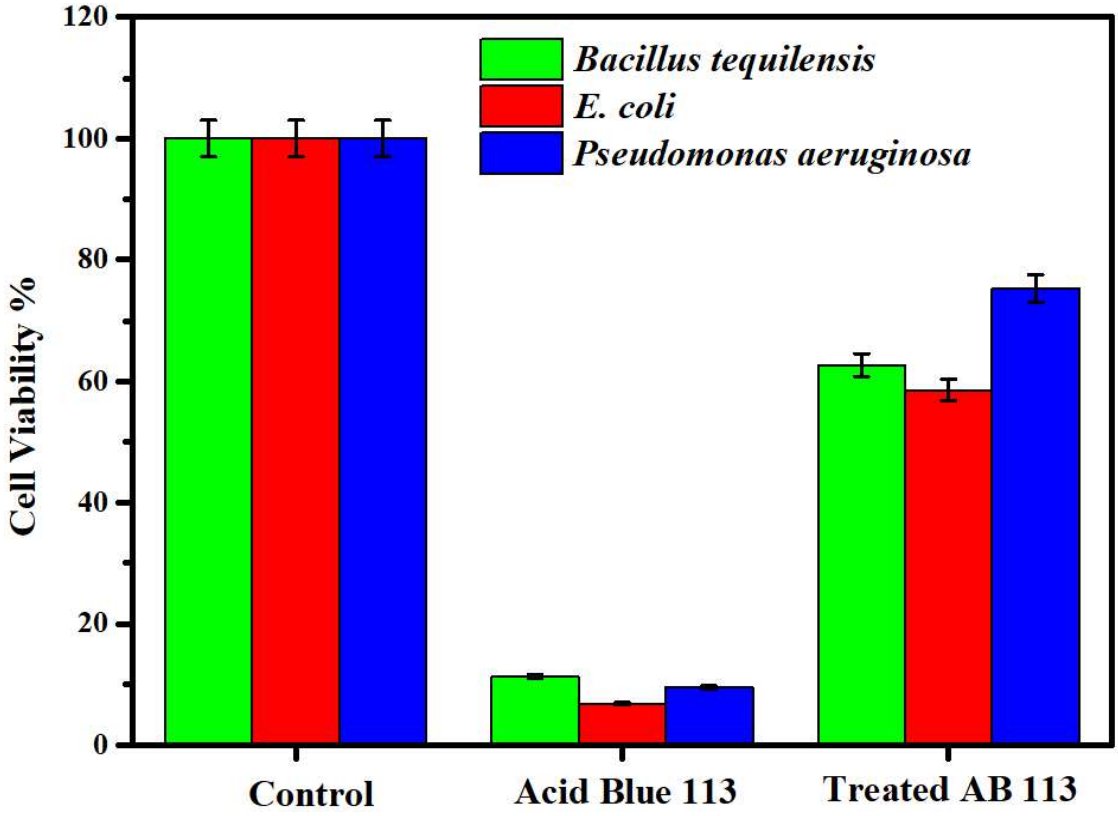

Figure 5.19. Quantifying the residual toxicity levels of AB 113 and its treated products using bacterial culture assays (Error bars depicted the standard deviation of triplicate study)

5.4 Conclusions

Graphene and its related nanostructured materials (Graphene Oxide) can act as hosts for microbial species, creating a synergistic system that is highly effective, stable, and versatile. In this study, KG-GO-CA hydrogel beads for the degradation of Acid Blue 113 dye in FBBR were investigated. The combination of adsorption and biodegradation demonstrates exceptional catalytic effectiveness. The hydrogel beads exhibited a maximum elimination capacity of 62.4 mg/L.day and 70.8% removal efficiency at an inlet shock loading rate of 100 mg/L.day. The effectiveness of the hydrogel beads was also observed over multiple cycles with a dye removal efficiency of 70.6 ± 2.5%. The adsorption isotherm study suggested that Langmuir isotherm was the most suitable model for describing the adsorption process. The toxicity assessment using three bacterial strains (*Bacillus tequilensis*, *E. coli*, and *Pseudomonas*

aeruginosa) indicated that the treated dye showed significantly higher cell viability and low toxicity. It can be concluded that the use of KG-GO-CA hydrogel beads in an FBBR system was an efficient and eco-friendly technique for the removal of Acid Blue 113 dye from wastewater.